https://doi.org/10.1016/j.compscitech.2022.109771

High Ionic Thermopower in Flexible Composite Hydrogel for Wearable Self-powered Sensor

Jingfei Zhang[a], Wei Xue[b], Yongqiang Dai[a], Bin Li[a], Yizhong Chen[a], Bing Liao[a, *], Wei Zeng[a, *], Xiaoming Tao[c] and Mingqiu Zhang[d]

[a] Flexible Sensing Technology Research Center, Guangdong Provincial Key Laboratory of industrial surfactant, Institute of Chemical Engineering, Guangdong Academy of Sciences, Guangzhou, China

[b] Department of Biomedical Engineering, Jinan University, Guangzhou, China

[c] Research Institute for Intelligent Wearable Systems, The Hong Kong Polytechnic University, Hong Kong

[d] Key Laboratory for Polymeric Composite and Functional Materials of Ministry of Education, Sun Yat-Sen University, Guangzhou, China

E-mail: liaobing@gic.ac.cn; zengwei@gdcri.com

Abstract

Ionic-conductive hydrogel sensors are widely used in wearable electronics, and biomedical monitoring. Meanwhile, the hydrogel can use the heat continuously released from human body to generate thermal voltage by relying on the thermal diffusion effect and achieving thermoelectric conversion. It is the most effective solution to realize self-powered supply obtaining energy from environmental waste heat. However, the low thermoelectric output power of hydrogel restricts their

applications. Herein, a highly flexible composite hydrogel with ultrahigh thermoelectric output power is designed, wherein hydrogel containing NaCl is prepared by radical polymerization and metal ion complexation, in which the $CaCl_2$ provide the second crosslinking network. Consequently, the optimized hydrogel has excellent stretchability and can withstand up to 1500% tension. The sensitivity of the hydrogel sensor is up to 7.01 in the range of 600%~1500%, which has excellent stability and reversibility. Furthermore, the fast response time of the hydrogel sensor was 12.8 ms. The ionic thermovoltage and power density observed in this study are 34.27 $mV \cdot K^{-1}$ and 730 $mW \cdot m^{-2}$, respectively. The results demonstrated that the ionic-conductive hydrogels with excellent ionic thermovoltage and the ultrahigh power density may be a potential candidate to realize the self-powered performance of hydrogel wearable sensor.

Keywords

Composite hydrogel, Wearable sensors, Self-powered, Ionic-conductive, Ionic thermovoltage

1. Introduction

Flexible and self-powered strain sensors are emerging as a promising new technology for next-generation wearable electronics duo to their tremendous potential in smart home, health detection, electronic skins and intelligent robotics. [1-7] Different from the traditional strain sensors which are limited in applications of large strain range because of the unstable conductivity under large strains and the low fracture strain caused by the poor compatibility between conductive filler and elastic matrix and the inherent brittleness of inorganic conductive materials,[8-10] the wearable strain sensors must meet the requirements of the mechanical properties including not only gentle flexing also strong deformations of rolling and stretching.[11-13] Furthermore, the flexibility, durability, stability, portability, high sensitivity as well as self-powered generation ability are essential requirements for the wearable sensors. [1, 14, 15] Until now, it is a challenging task to reasonably design a multifunctional flexible sensor with the above characteristics.

To achieve high performance wearable strain sensors, various flexible conducting materials using as the strain sensor have been explored, in which conducting materials such as MXene, carbon nanotubes, graphene, metallic nanomaterials are combined with elastomers. Despite the enormous progress made in this emerging field, the integration of wide sensing range and great sensitivity into flexible strain sensors is still a significant challenge. As an alternative, conductive hydrogels with excellent mechanical and electrical properties have been identified as excellent alternative materials for wearable or implantable devices due to their good

biocompatibility, high flexibility and stable conductivity even under large strain[13, 15-20]. For examples, Wang et al.[21] prepared a hydrogel with thermal response and electrical conductivity using poly(N-isopropylacrylamide) as the heat-sensitive material and polyaniline (PANI) as the conductive material. However, organic solvents were used in the preparation process because of the insolubility of PANI in water, which was unfriendly to the environment and limited the application of hydrogel in the body. The composite hydrogels above prepared with the conductive materials (metal nanowires, graphene, PANI) [22, 23] cannot achieve high conductivity and optical transparency simultaneously and exhibit poor biocompatibility, causing the limitation of the applications. In order to resolve the insolubility of conductive materials in hydrogels, polyelectrolytes or salts (lithium chloride, sodium chloride) were usually added into the system to realize the conductivity through ion transport. [24, 25]

More importantly, current sensing systems still require external power supplies to achieve efficient operation of the device, the existing batteries have a limited service life and need to be replaced or recharged frequently, making them unsuitable for long-time unattended monitoring and largely restricting their wide application in wearable sensors. How to harvest energy from abundant environmental energy even the human body is a critical issue for the wearable sensor used to monitor human health.[26, 27] In order to further investigate of self-powered wearable sensors, great efforts have been focused on solar cells, piezoelectric, triboelectric and thermoelectric generators (TEGs), which can harvest energy from surrounding environment or

human body.[28-31] Among them, TEGs with the advantage of reliability can transform the continuously released body heat into reliable renewable energy, providing a reasonable solution for the power supply of most sensors.[26, 32-34] The main working principle of ionic-conductive hydrogels to achieve thermoelectric transformation is thermal diffusion effect.[27] Anions and cations dispersed directionally to the hot ends and cold ends of the hydrogel, respectively, in the presence of temperature gradient, and then aggregated on both sides of electrodes to produce ion concentration difference and corresponding thermal voltage.[27, 35] The thermoelectric generators based on the ion-conductive hydrogel combine the merits of excellent mechanical and electrical properties as well as thermoelectric voltage, which are suitable for self-powered wearable flexible sensor.

Herein, we propose a self-powered flexible sensor based on ionic-conductive double network (DN) hydrogel, in which a single network (SN) hydrogel was firstly obtained by radical polymerization and DN structure was further formed by coordination complexation. Sodium chloride (NaCl) was introduced as a conductive ion. The hydrogel sensor can achieve high sensitivity detection in a wide response range of 1500% and the gauge factor (GF) is up to 7.01. Furthermore, the hydrogel can effectively convert low grade waste heat into electrical energy attribute to the thermal diffusion effect in the presence of temperature gradient, with an ultrahigh ionic thermovoltage of 34.27 $mV \cdot K^{-1}$, a high current density of 4.49 $A \cdot m^{-2}$ and a maximum power density of 730 $mW \cdot m^{-2}$. Further, the sensor exhibited mechanical flexibility and great thermoelectric potential which provide an effective solution to

realize the self-powered performance of hydrogel wearable sensor.

2. Results and discussion

The DN ion-conductive hydrogel with high sensitivity, excellent stretchability and thermoelectric properties was synthesized by a two-step combination as shown in Fig. 1a. The first chemically cross-linked network was formed through free radical polymerization of sodium acrylate (AANa) and acrylamide (AM) in which the NaCl was introduced as conductive ions. Thereafter, reversible ionic crosslinking points were formed between sodium alginate (SA) and Ca^{2+} through immersing SN hydrogel in $CaCl_2$ solution, which facilitates the high strength of the hydrogel. The DN hydrogel prepared was named SA/P(AM-AANa)/$CaCl_2$. Moreover, the broken coordination bonds can also be combined again under certain conditions, giving the hydrogel excellent self-recovery performance and energy dissipation.[36] The FT-IR measurement results of DN ion-conductive hydrogel are presented in Fig. 1b to indicate the successful preparation of hydrogels. It can be seen that the peaks of AM at 1280 cm^{-1} and 1610 cm^{-1} were respectively generated by the flexural vibration of C-H of the C=C bond and the stretching vibration of C=C. The above peaks disappeared in the FT-IR spectrum of the DN hydrogel, showing the cross-linking polymerization between AM and AANa. Besides, the peaks of SA at 1415 cm^{-1} and 1610 cm^{-1} belong to the symmetric stretching vibration and the asymmetric stretching vibration of -COO-, which separately shifts to 1627 cm^{-1} and 1416 cm^{-1} in the DN hydrogel, indicating that the -COOH is complexed with Ca^{2+} to form the second network. These above results show that the DN hydrogel was synthesized successfully

through free radical polymerization and the coordination complexation. Further, the transmission of the hydrogel was measured with an UV-Vis and the light transmittance is 90.08% (Fig. 1c). Compared with the conductive hydrogels prepared with carbon-based materials, the high-transparency conductive hydrogel prepared in this work could greatly broaden the application range of conductive hydrogels and are especially suitable for some fields that require higher optical performance, such as display equipment and light-emitting devices, etc.

The effect of crosslinker content on the mechanical properties of hydrogel was also investigated as demonstrated in Fig. S1. The break elongation, tensile strength and toughness decreased with the increasing content of the crosslinker, which could be attributed to that higher crosslinking density of the hydrogel was formed with increasing the content of the crosslinker, more energy was needed to move the molecular chain when the hydrogel was stretched, resulting a limited stretchability of the chain segment and the increase of Young's modulus. Besides, the effect of the immersing time on cross-linking between SA and Ca^{2+} was illustrated in Fig. S1d. The tensile strength of hydrogel increased while the break elongation decreased after immersing the SN hydrogel in Ca^{2+} solution to form the second network, which could be attributed to the reversible ionic crosslinking points were formed between SA and Ca^{2+}, resulting the more tightly network with the increasing of the immersing time. The results indicate that the cross-linking between SA and Ca^{2+} can greatly increase the strength of the composite hydrogel without an extreme reduction of the flexibility with the immersing time of 15 seconds. Further decreasing the crosslinker content

was unable to form a stable hydrogel, therefore, the hydrogel with 0.03% crosslinker content was selected as the optimized sample. Notably, the optimized DN hydrogel has excellent stretchability and can withstand up to 1500% of tensile without breakage (Fig. S1a). The morphologies of SN hydrogel and DN hydrogel were described by SEM as shown in Fig. S2 and Fig. 1d, respectively. Compared with the morphology of SN hydrogel, the DN hydrogel presented a more tightly network after immersing the SN hydrogel in Ca^{2+} solution to form the second network, indicating the generation of ionic network through coordination complexation. The porous structure of hydrogel provides channels for ion transportation to achieve the excellent conductivity and thermal voltage.

The self-powered strategy of ionic-conductive hydrogels is thermoelectric transformation through thermal diffusion effect.[27] Sodium ions and chloride ions respectively accumulate on the cold side and hot side in the presence of temperature difference to produce ion concentration difference, thus generating a thermo voltage.[27, 35] The thermoelectric performance analysis of DN hydrogel is shown in Fig. 2. The output voltages of ionic-conductive hydrogel at different temperature gradient (ΔT) were measured as illustrated in Fig. 2a,b. The output voltage increased proportionally with the increasing of the applied ΔT and exhibited a stable response at constant ΔT. The voltage even reached as high as 518.8 mV at the ΔT of 15 K. The ionic thermovoltage of 34.27 $mV \cdot K^{-1}$ was obtained through the slope between the output voltage and the temperature gradient, which is one of the highest thermal voltages for ionic TE materials with such excellent flexibility. In addition, the

current-voltage and power-voltage curves at ΔT of 5K, 10K, and 15K were also investigated as shown in Fig. 2c. The ionic-conductive hydrogel produced a high current density of 4.49 $A \cdot m^{-2}$ at the ΔT of 15 K and the corresponding power density of 730 $mW \cdot m^{-2}$, which was higher than most of the ionic thermoelectric materials reported in literatures, as illustrated in Fig. 2d and Table S1. The ionic conductivity (σ) and thermal conductivity (κ) of hydrogel were also measured in order to further characterize the thermoelectric properties, as presented in Fig. 2e. The value of σ and κ are respectively 0.29~0.59 $S \cdot m^{-1}$ and 0.5359~0.5522 $W \cdot m^{-1} \cdot K^{-1}$ in the temperature range of 278 ~298 K. Furthermore, the corresponding ionic ZT_i was also calculated by the following formula, $ZT_i = S_i^2 \sigma T/\kappa$, where S_i is ionic thermovoltage ($V \cdot K^{-1}$), σ is ionic conductivity ($S \cdot m^{-1}$), κ and T are separately thermal conductivity ($W \cdot m^{-1} \cdot K^{-1}$) and absolute temperature (K) [26, 27]. The value of ZT_i are 0.19~0.36 in the temperature range of 278 ~298 K. Besides, the power factor (PF_i) can be obtained by the following equation, $PF_i = S_i^2 \sigma$, which was generally used to evaluate the thermoelectric properties. The PF_i of 0.30~0.70 $mW \cdot m^{-1} \cdot K^{-2}$ was shown in Fig. S3a. In addition, the stability of the thermoelectric properties of the hydrogel needed to be considered. The output voltage for a long duration was measured as shown Fig. 2f, which maintained basically stable under the constant ΔT of 15K for at least 22 hours. The long-term stability of output voltage will be necessary to ensure that the TE hydrogels are suitable for long-term unattended monitoring operation. The hydrogel with excellent TE properties above were usually used in the ionic thermoelectric capacitors for thermoelectric conversion. Fig. 2g illustrates voltage profile of the three

stages for the TE hydrogel loaded with 5 kΩ external resistor. Firstly, the temperature gradient of 7.5 K was applied to the TE hydrogel, inducing the accumulations of the Na^+ and Cl^- at the cold side and the hot side, respectively, and then generating the corresponding thermal voltage of 273 mV, which is called stage I of thermo-ionic charging. When the external resistor of 5 kΩ was loaded with the TE hydrogel, there will be current passing through the external load to balance the voltage generated by the ions, producing a decrease of the voltage, [34, 37] which is known as stage II, discharge process. In the stage III, the output voltage continued to decrease to 0 when the temperature difference of thermoelectric hydrogel was eliminated due to the ions in thermoelectric hydrogels return to their initial state.

Besides, the stability of the voltage generated by hydrogels during the repeated circuit opening and loading cycles (5 kΩ) was also measured. The voltage of 0.53 V was firstly achieved at a constant ΔT of 15K and then decreased to 0.07 V when the external resistor of 5 kΩ was loaded with the TE hydrogel, which was almost restored to the initial value while disconnecting the external resistance, as shown in Fig. S3b. The output voltage exhibits good thermoelectric repeatability with little degradation during the cycles. These excellent thermoelectric properties aforementioned of the hydrogels provide the potential application in wearable self-powered sensors.

Subsequently, the performance of the ion-conductive hydrogel-based sensor was investigated to confirm its suitability for wearable flexible sensors. Fig. 3a shows the I-V characteristics of hydrogel under different tensile strains from 100% to 500%. The current of hydrogel increased linearly with the increase of voltage, indicating that

hydrogel has good ohmic characteristics. Besides, the slope of the I-V curve decreased with the increase of tensile strain. According to Ohm's law, the I-V curve slope is inversely proportional to the resistance, [38, 39] indicating that the resistance of the hydrogel increased accordingly with increasing strain. This was because the conductivity mainly depended on the transportation of conducting ions of the hydrogel, the average distance between ions gradually increased during stretching, thus increasing the resistance. The performance of the DN hydrogel was investigated when tensile strain was applied continuously. As shown in Fig. 3b, $\Delta R/R_0$ value increases with the increase of the strain. It is because the conductive path changes more significantly with the increase of the strain, resulting in more pronounced changes of relative resistance.[40-42] The relative resistance change increased to 8933% at the strain of 1461%, where the hydrogel strain sensor exhibited a high GF of 6.11. It can be seen that the sensitivity is higher in the large strain range, which is caused by the decrease of the continuity of conductive ions in the stretching direction due to the elongation of the hydrogel network when stretching the hydrogel strain sensor. The continuity of conductive ions decreased more obviously with the increase of the strain, resulting in larger $\Delta R/R_0$ values and higher sensitivity. Besides, the sensitivity for different strain intervals was obtained respectively, showing a good linear response for each strain interval. It's worth noting that the GF was 3.25 in the lower strain range (0~300%), further increased to 6.82 (300 ~ 600%) and 7.01 (600 ~ 1500%) respectively with increasing the strain range, which is much higher than that of strain sensors based on hydrogel (GF =0.478,[43] 0.63,[41] 0.84,[44] 1.32,[45] 1.51,[22]

1.54,[46], 1.58,[40] 2.10[25], 3.15[47] 2.2,[7] 2.42,[12] 2.48,[13] 9.89,[6] 14.6, [11]) (Fig. 3c).

In addition, Fig. 3d illustrated the response time of 12.8 ms of the DN hydrogel sensor, which was measured under instantaneous tensile deformation, the fast response time made it possible to monitor a series of motion signals in a real time.

To further confirm the stability and reliability of the sensor, the performances of the hydrogel-based sensor during the loading-unloading cycles under various strains from 10% to 400% were also explored. Fig. 4a shows similar and stable waveforms during the cycles at the same strain, and the $\Delta R/R_0$ value increased with increasing strain, indicating the excellent sensing performance and good repeatability. Furthermore, Fig. 4b displays the sensing performance of hydrogel when the strain increases step by step. Similarly, the $\Delta R/R_0$ value of the sensor increased gradually with the increase of strain and was basically stable under a fixed strain. In addition, the value can be basically recovered with the recovery of strain due to the elasticity of hydrogel, indicating that the sensor with high sensitivity, reversibility and stability. The performances of hydrogel-based sensor were related to the resistance change, that is, the distance change between the ions during the stretching process, as displayed in Fig. S4. Specifically, the conductivity of the DN hydrogel depended mainly on the transportation of conducting ions in the porous network. The distance between ions increased with increasing the tensile strain, leading an increase of resistance. The distance between the ions was then returned to the initial state in the hydrogel restoration process, leading the recovery of conduction path. Furthermore, as

presented in Fig. 4c, when different voltages (0.01 ~1 V) are applied, the DN hydrogel sensor shows stable response signals. Furthermore, the sensors can still generate stable and effective response signal even a voltage as low as 0.01V was applied, implying the independence of the sensitivity on the applied voltages. Notably, such a low voltage operating environment makes it possible to prepare sensors for portable wearable devices. Meanwhile, the responses of hydrogel sensor have no dependence on the tensile speed (100~500 mm·min^{-1}) in the applied strain range as depicted in Fig. 4d, showing that the hydrogel-based sensor can be well suited to a wide range of tensile speeds. In addition to the excellent tensile properties mentioned above, Fig. 4e displays the compressive sensing performances of hydrogel sensors under cyclic compression from 20% to 80%, showing high sensitivity and stability. The ion concentration per unit length of hydrogel system increased when pressing, resulting in high sensing signal (Fig. S4). More importantly, the sensor demonstrated its excellent stability and durability through 6,000 loading/unloading cycles at 20% compressive strain as shown in Fig. 4f. Besides, the sensing performance of the hydrogel after being sealed and stored at room temperature for 30 days, the break elongation and sensitivity of the hydrogel sensor were not significantly reduced, indicating its good environmental stability (Fig. S5).

The hydrogel could be used in monitoring human motions due to the unique flexibility, excellent sensitivity and fast response time. Fig. 5a,b show the performances of the hydrogel-based sensor attached to the finger and the elbow, respectively. The responsiveness of the hydrogel sensor increased with the increase in

curvature degree of the finger and the elbow and could be remained stable at the same curvature degree, meanwhile, it returns to its original state when the joint was straightened and relaxed. In addition, the sensor was stretched and compressed when the wrist was bent downward and upward, respectively, resulting reversed response values as illustrated in Fig. 5c. Similarly, as shown in Fig. 5d, when the sensor was fixed to the abdomen to monitor the signal generated by human breathing, it can be found that the compression degree of the hydrogel sensor varies with the depth of breathing, resulting in the different response values. Furthermore, the response of hydrogel sensor for pulse monitoring was showed in Fig. S6, implying the high sensitivity of sensor. Moreover, the performances were tested when the finger respectively singly-pressed or doubly-pressed on sensor surface to gain insight into the behavior of hydrogel sensor. As illustrated in Fig. 5e, the number of sensing peak is consistent with the pressing number of finger. In addition, as demonstrated in Fig. 5f, the hydrogel sensor showed corresponding peak signals, when the letters of A, C and M were written on the surface of the hydrogel sensor. The above results indicate that the hydrogel sensor has excellent sensitivity, repeatability and stability, which shows great potential for application in monitoring human motions.

In addition to the above tests on the sensing performances of the hydrogel when external power was applied, the sensing behaviors based on its self-powered characterization were also investigated. Firstly, the variations of open circuit voltage in the thermoelectric hydrogel at the ΔT of 7.5 K were analyzed when different compression strains were applied. Fig. S7 illustrated the corresponding equivalent

circuit diagram. The voltage of 228 mV was obtained for the TE hydrogel at the ΔT of 7.5 K, and then different compressive strains were applied to the TE hydrogel, causing a decrease of the open circuit voltage as illustrated in Fig. 6a. The open voltage decreases with increasing compressive strain which shows a self-powered sensing performance. Here, the ionic conductor-based hydrogel thermoelectric device can be treated as a capacitor whose capacitance value depends on the distance between the electrodes and the electrode area ($C= \varepsilon S/4\pi kd= Q/V$), the thermoelectric device is compressed thereby reducing the distance (d) between the two electrodes of the capacitor when the electrode area is constant. And the output open-circuit voltage of this capacitor decreases almost linearly with the distance between the electrode plates under the condition of constant temperature difference. The voltage variation with the compressive strain was shown in the inset Fig.. In particular, to demonstrate the self-powered characteristics of this ion-conductive hydrogel and its self-powered sensing performance, we constructed a self-powered sensing system with a hybrid hydrogel sensor/hydrogel thermoelectric device system driven entirely by thermoelectric power rather than by an external power source (Fig. S8). Firstly, the open circuit voltage of hydrogel reached to a stable value of 228 mV at ΔT of 7.5 K (stage I). Then the TE hydrogel was connected in parallel with the strain sensor (stage II), which was similar to the external resistor, causing the rapid decrease of the voltage to 3.7 mV in stage II as shown in Fig. 6b. The corresponding equivalent circuit diagram of the self-powered ionic-conductive hydrogel is shown in Fig. 6c. Afterwards, the flexible sensor was firstly pre-stretched to 500% (stage III), and then

cyclic loaded-unloaded under the strains of 20% and 40% (stage IV). According to the formula, $V_s = V_0/(R+R_s)*R_s$, where V_s is the voltage applied on the sensor, V_0 is the thermoelectric voltage generated by the ionic-conductive hydrogel, R_s and R are the resistance of the sensor and the internal resistance of the TE hydrogel, respectively. In stage III and IV, when the tensile strain was applied, R_s of the sensor increased, generating an increase in the voltage V_s of the sensor. Therefore, the voltage across the sensor increased with increasing strain and showed similar and stable waveforms during the cycles under the same strain, indicating the excellent sensing performance and good repeatability as shown in Fig. 6b. Therefore, the strain changes caused by external stimuli can be characterized by the voltage changes without external power supply, which provides an effective solution for achieving the self-powered performance of thermoelectric hydrogels.

3. Conclusions

In summary, ionic-conductive DN hydrogel prepared by situ polymerizations and coordination complexation exhibits excellent stretchability of 1500%, high sensitivity (GF=7.01), and fast response time of 12.8 ms. The hydrogel sensor with excellent sensing stability and reliability can be applied to detect human motion precisely. Importantly, the ionic-conductive hydrogel can form a stable thermal voltage by the ions thermal diffusion effect in the presence of temperature gradient, which exhibits a giant ionic thermovoltage of 34.27 $mV \cdot K^{-1}$ and a ultrahigh power density of 730 $mW \cdot m^{-2}$. Besides, the ZT_i value of the hydrogel reaches to 0.36. The thermoelectric hydrogel can be used as ionic thermoelectric capacitors or self-powered devices for

other sensors to detect external stimuli without the need for external voltages. This work demonstrates that ionic-conductive DN hydrogel exhibited excellent sensing performance and great thermoelectric potential, providing an effective solution to realize the self-powered performance of hydrogel wearable sensor.

Declaration of Competing Interest

The authors declare that they have no known competing financial interests or personal relationships that could have appeared to influence the work reported in this paper.

Acknowledgements

This work was supported by the National Natural Science Foundation of China (NO. 52073066), the GDAS' Project of Science and Technology Development (NO. 2021GDASYL-20210103094, NO. 2020GDASYL-20200102028), Guangdong Basic and Applied Basic Research Foundation (NO. 2022A1515010685).

Reference

[1] C. Zhao, Y. Wang, G. Tang, J. Ru, Z. Zhu, B. Li, C.F. Guo, L. Li, D. Zhu, Ionic flexible sensors: Mechanisms, materials, structures, and applications, Adv. Funct. Mater. 32(17) (2022) 2110417.

[2] M. Yue, Y. Wang, H. Guo, C. Zhang, T. Liu, 3D reactive printing of polyaniline hybrid hydrogel microlattices with large stretchability and high fatigue resistance for wearable pressure sensors, Compo. Sci. Technol. 220 (2022).

[3] Y. Wu, S. Sun, A. Geng, L. Wang, C. Song, L. Xu, C. Jia, J. Shi, L. Gan, Using tempo-oxidized-nanocellulose stabilized carbon nanotubes to make pigskin hydrogel

conductive as flexible sensor and supercapacitor electrode: Inspired from a chinese cuisine, Compo. Sci. Technol. 196 (2020).

[4] K. Feng, G.-Y. Hung, X. Yang, M. Liu, High-strength and physical cross-linked nanocomposite hydrogel with clay nanotubes for strain sensor and dye adsorption application, Compo. Sci. Technol. 181 (2019).

[5] Z. Zhou, C. Qian, W. Yuan, Self-healing, anti-freezing, adhesive and remoldable hydrogel sensor with ion-liquid metal dual conductivity for biomimetic skin, Compo. Sci. Technol. 203 (2021).

[6] C. Zhang, M. Wang, C. Jiang, P. Zhu, B. Sun, Q. Gao, C. Gao, R. Liu, Highly adhesive and self-healing γ-PGA/PEDOT:PSS conductive hydrogels enabled by multiple hydrogen bonding for wearable electronics, Nano Energy 95 (2022).

[7] J. Wang, T. Dai, Y. Zhou, A. Mohamed, G. Yuan, H. Jia, Adhesive and high-sensitivity modified $Ti_3C_2T_X$ (Mxene)-based organohydrogels with wide work temperature range for wearable sensors, J. Colloid Interface Sci. 613 (2022) 94-102.

[8] D. Qi, K. Zhang, G. Tian, B. Jiang, Y. Huang, Stretchable electronics based on PDMS substrates, Adv. Mater. 33(6) (2020) 2003155.

[9] X.G. Yu, Y.Q. Li, W.B. Zhu, P. Huang, T.T. Wang, N. Hu, S.Y. Fu, A wearable strain sensor based on a carbonized nano-sponge/silicone composite for human motion detection, Nanoscale 9(20) (2017) 6680-6685.

[10] X. Sun, Z. Qin, L. Ye, H. Zhang, Q. Yu, X. Wu, J. Li, F. Yao, Carbon nanotubes reinforced hydrogel as flexible strain sensor with high stretchability and mechanically toughness, Chem. Eng. J. 382 (2020) 122832.

[11] H. Zhang, H. Shen, J. Lan, H. Wu, L. Wang, J. Zhou, Dual-network polyacrylamide/carboxymethyl chitosan-grafted-polyaniline conductive hydrogels for wearable strain sensors, Carbohyd. Polym. 295 (2022) 119848.

[12] H. Huang, X. Zhang, Z. Dong, X. Zhao, B. Guo, Nanocomposite conductive tough hydrogel based on metal coordination reinforced covalent pluronic f-127 micelle network for human motion sensing, J. Colloid Interface Sci. 625 (2022) 817-830.

[13] M. Wu, X. Wang, Y. Xia, Y. Zhu, S. Zhu, C. Jia, W. Guo, Q. Li, Z. Yan, Stretchable freezing-tolerant triboelectric nanogenerator and strain sensor based on transparent, long-term stable, and highly conductive gelatin-based organohydrogel, Nano Energy 95 (2022).

[14] Q. Wang, X. Pan, C. Lin, X. Ma, S. Cao, Y. Ni, Ultrafast gelling using sulfonated lignin-Fe^{3+} chelates to produce dynamic crosslinked hydrogel/coating with charming stretchable, conductive, self-healing, and ultraviolet-blocking properties, Chem. Eng. J. 396 (2020) 125341.

[15] P. Shi, Y. Wang, K. Wan, C. Zhang, T. Liu, A waterproof ion-conducting fluorinated elastomer with 6000% stretchability, superior ionic conductivity, and harsh environment tolerance, Adv. Funct. Mater. (2022) 2112293.

[16] Y. Zhu, J. Liu, T. Guo, J.J. Wang, X. Tang, V. Nicolosi, Multifunctional $Ti_3C_2T_X$ Mxene composite hydrogels with strain sensitivity toward absorption-dominated electromagnetic-interference shielding, ACS Nano 15(1) (2021) 1465-1474.

[17] Y. Yang, Y. Yang, Y. Cao, X. Wang, Y. Chen, H. Liu, Y. Gao, J. Wang, C. Liu, W. Wang, J.-K. Yu, D. Wu, Anti-freezing, resilient and tough hydrogels for sensitive and large-range strain

and pressure sensors, Chem. Eng. J. 403 (2021) 126431.

[18] X. Li, L. He, Y. Li, M. Chao, M. Li, P. Wan, L. Zhang, Healable, degradable, and conductive mxene nanocomposite hydrogel for multifunctional epidermal sensors, ACS Nano 15(4) (2021) 7765-7773.

[19] J. Zhang, W. Xue, Y. Dai, L. Wu, B. Liao, W. Zeng, X. Tao, Double network hydrogel sensors with high sensitivity in large strain range, Macromol. Mater. Eng. 306(12) (2021) 2100486.

[20] J. Ren, Y. Liu, Z. Wang, S. Chen, Y. Ma, H. Wei, S. Lü, An anti-swellable hydrogel strain sensor for underwater motion detection, Adv. Funct. Mater. 32(13) (2021) 2107404.

[21] Z. Wang, H. Zhou, W. Chen, Q. Li, B. Yan, X. Jin, A. Ma, H. Liu, W. Zhao, Dually synergetic network hydrogels with integrated mechanical stretchability, thermal responsiveness, and electrical conductivity for strain sensors and temperature alertors, ACS Appl. Mater. Interfaces 10(16) (2018) 14045-14054.

[22] G. Cai, J. Wang, K. Qian, J. Chen, S. Li, P.S. Lee, Extremely stretchable strain sensors based on conductive self-healing dynamic cross-links hydrogels for human-motion detection, Adv. Sci. 4(2) (2017) 1600190.

[23] L. Hsiao, L. Jing, K. Li, H. Yang, Y. Li, P. Chen, Carbon nanotube-integrated conductive hydrogels as multifunctional robotic skin, Carbon 161 (2020) 784-793.

[24] Y. Yang, L. Guan, X. Li, Z. Gao, X. Ren, G. Gao, Conductive organohydrogels with ultrastretchability, antifreezing, self-healing, and adhesive properties for motion detection and signal transmission, ACS Appl. Mater. Interfaces 11(3) (2019) 3428-3437.

[25] W. Hou, N. Sheng, X. Zhang, Z. Luan, P. Qi, M. Lin, Y. Tan, Y. Xia, Y. Li, K. Sui, Design of injectable Agar/NaCl/polyacrylamide ionic hydrogels for high performance strain sensors,

Carbohyd. Polym. 211 (2019) 322-328.

[26] Z. Fan, D. Du, X. Guan, J. Ouyang, Polymer films with ultrahigh thermoelectric properties arising from significant seebeck coefficient enhancement by ion accumulation on surface, Nano Energy 51 (2018) 481-488.

[27] H. Cheng, J. Ouyang, Ultrahigh thermoelectric power generation from both ion diffusion by temperature fluctuation and hole accumulation by temperature gradient, Adv. Energy Mater. 10(37) (2020) 2001633.

[28] Yaling Wang, Wei Zhu, Yuan Deng, Bo Fu, Pengcheng Zhu, Yuedong Yu, Jiao Li , J. Guo, Self-powered wearable pressure sensing system for continuous healthcare monitoring enabled by flexible thin-film thermoelectric generator, Nano Energy 73 (2020) 104773.

[29] N. Wen, Z. Fan, S. Yang, Y. Zhao, T. Cong, S. Xu, H. Zhang, J. Wang, H. Huang, C. Li, L. Pan, Highly conductive, ultra-flexible and continuously processable PEDOT:PSS fibers with high thermoelectric properties for wearable energy harvesting, Nano Energy 78 (2020) 105361.

[30] L. Li, W.D. Liu, Q. Liu, Z.G. Chen, Multifunctional wearable thermoelectrics for personal thermal management, Adv. Funct. Mater. (2022) 2200548.

[31] Z. Liu, H. Cheng, H. He, J. Li, J. Ouyang, Significant enhancement in the thermoelectric properties of ionogels through solid network engineering, Adv. Funct. Mater. 32(7) (2021) 2109772.

[32] S. Panigrahy, B. Kandasubramanian, Polymeric thermoelectric PEDOT:PSS & composites: Synthesis, progress, and applications, Eur. Polym. J. 132 (2020) 109726.

[33] Y. Hao, X. He, L. Wang, X. Qin, G. Chen, J. Yu, Stretchable thermoelectrics: Strategies,

performances, and applications, Adv. Funct. Mater. 32(13) (2021) 2109790.

[34] Y. Fang, H. Cheng, H. He, S. Wang, J. Li, S. Yue, L. Zhang, Z. Du, J. Ouyang, Stretchable and transparent ionogels with high thermoelectric properties, Adv. Funct. Mater. 30(51) (2020) 2004699.

[35] H. Cheng, X. He, Z. Fan, J. Ouyang, Flexible quasi-solid state ionogels with remarkable seebeck coefficient and high thermoelectric properties, Adv. Energy Mater. 9(32) (2019) 1901085.

[36] Q. Zheng, L. Zhao, J. Wang, S. Wang, Y. Liu, X. Liu, High-strength and high-toughness sodium alginate/polyacrylamide double physically crosslinked network hydrogel with superior self-healing and self-recovery properties prepared by a one-pot method, Colloids Surf., A 589 (2020) 124402.

[37] X. Yang, Y. Tian, B. Wu, W. Jia, C. Hou, Q. Zhang, Y. Li, H. Wang, High-performance ionic thermoelectric supercapacitor for integrated energy conversion-storage, Energy Environ. Mater. 0 (2021) 1-8.

[38] X. Zhao, C. Hang, H. Lu, K. Xu, H. Zhang, F. Yang, R. Ma, J. Wang, D. Zhang, A skin-like sensor for intelligent braille recognition, Nano Energy 68 (2020) 104346.

[39] K. He, Y. Hou, C. Yi, N. Li, F. Sui, B. Yang, G. Gu, W. Li, Z. Wang, Y. Li, G. Tao, L. Wei, C. Yang, M. Chen, High-performance zero-standby-power-consumption-under-bending pressure sensors for artificial reflex arc, Nano Energy 73 (2020) 104743.

[40] H. Sun, Y. Zhao, C. Wang, K. Zhou, C. Yan, G. Zheng, J. Huang, K. Dai, C. Liu, C. Shen, Ultra-stretchable, durable and conductive hydrogel with hybrid double network as high performance strain sensor and stretchable triboelectric nanogenerator, Nano Energy 76 (2020)

105035.

[41] S. Liu, L. Li, Ultrastretchable and self-healing double-network hydrogel for 3D printing and strain sensor, ACS Appl. Mater. Interfaces 9(31) (2017) 26429-26437.

[42] G. Ge, Y. Zhang, J. Shao, W. Wang, W. Si, W. Huang, X. Dong, Stretchable, transparent, and self-patterned hydrogel-based pressure sensor for human motions detection, Adv. Funct. Mater. 28(32) (2018) 1802576.

[43] Y.J. Liu, W.T. Cao, M.G. Ma, P. Wan, Ultrasensitive wearable soft strain sensors of conductive, self-healing, and elastic hydrogels with synergistic "soft and hard" hybrid networks, ACS Appl. Mater. Interfaces 9(30) (2017) 25559-25570.

[44] K. Tian, J. Bae, S.E. Bakarich, C. Yang, R.D. Gately, G.M. Spinks, M. In Het Panhuis, Z. Suo, J.J. Vlassak, 3D printing of transparent and conductive heterogeneous hydrogel-elastomer systems, Adv. Mater. 29(10) (2017) 1604827.

[45] X. Jing, H. Mi, X. Peng, L. Turng, Biocompatible, self-healing, highly stretchable polyacrylic acid/reduced graphene oxide nanocomposite hydrogel sensors via mussel-inspired chemistry, Carbon 136 (2018) 63-72.

[46] T. Li, Y. Wang, S. Li, X. Liu, J. Sun, Mechanically robust, elastic, and healable ionogels for highly sensitive ultra-durable ionic skins, Adv. Mater. 32(32) (2020) 2002706.

[47] T. Zhu, Y. Cheng, C. Cao, J. Mao, L. Li, J. Huang, S. Gao, X. Dong, Z. Chen, Y. Lai, A semi-interpenetrating network ionic hydrogel for strain sensing with high sensitivity, large strain range, and stable cycle performance, Chem. Eng. J. 385 (2020) 123912.

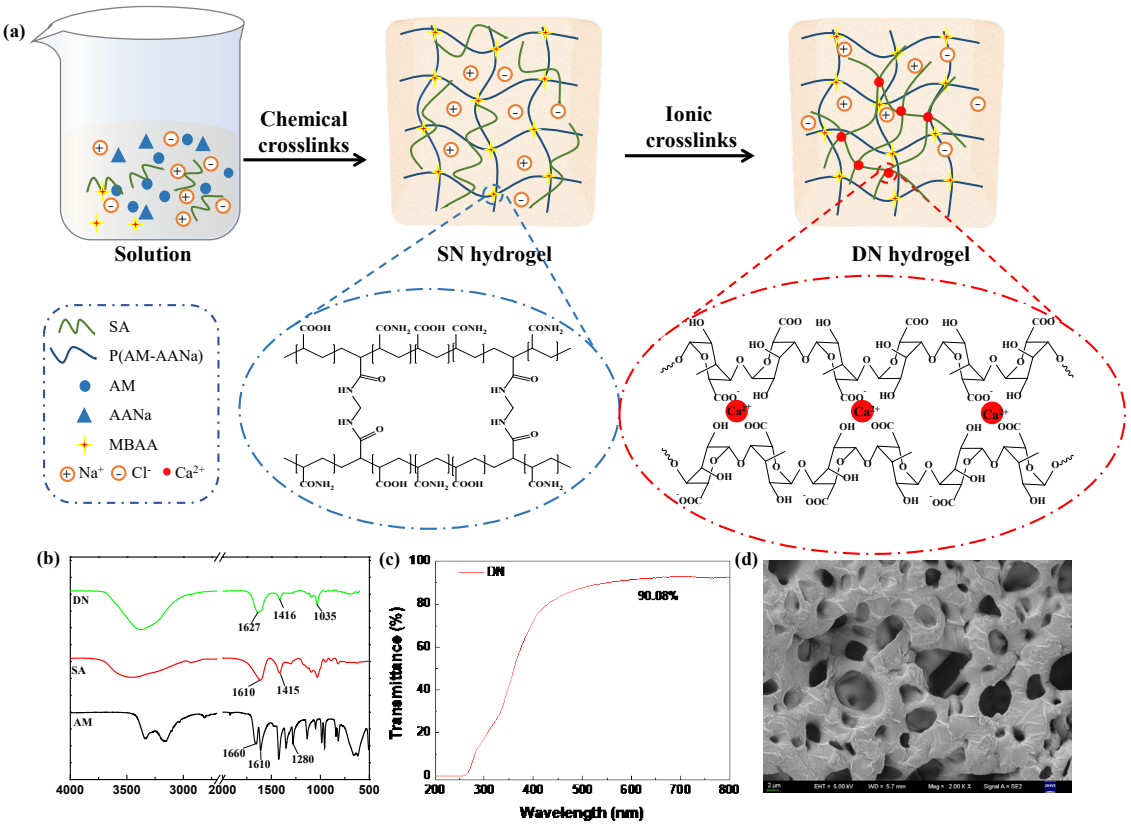

Fig. 1. a) Synthesis schematic of the DN hydrogel. b) FT-IR spectra of the SA, AM and DN hydrogel. c) UV-Vis spectra of the DN hydrogels. d) The SEM image of freeze-dried DN hydrogel.

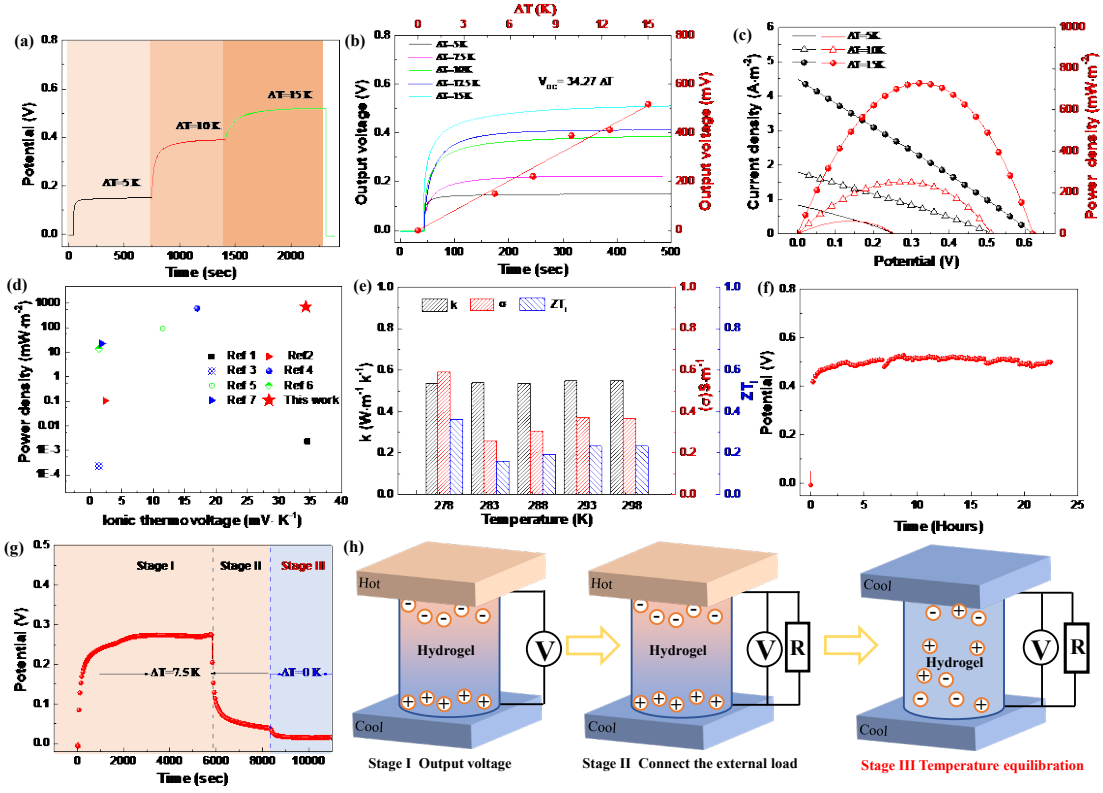

Fig. 2. a) The output voltage with respect to the temperature gradient and b) the corresponding ionic thermovoltage. c) Current-voltage and power-voltage curves of the TE hydrogel at ΔT of 5K, 10K, and 15K. d) Comparison of ionic thermovoltage and power density with those reported ionic thermoelectric materials. e) Temperature dependence of thermal conductivity, ionic conductivity and ionic ZT_i. f) The long term stability of output voltage generated by TE hydrogel at a constant ΔT of 15K. g) Voltage profiles of the ionic TE hydrogel capacitors connected with external resistor and h) the corresponding illustration of the working principles.

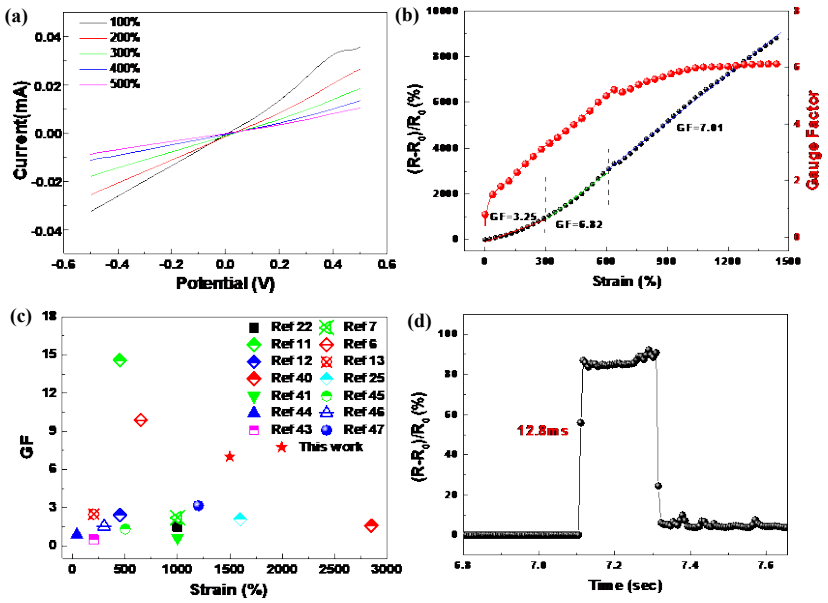

Fig. 3. a) Current-voltage curves under different tensile strains. b) Relative resistance changes and GFs of the hydrogel sensor to continuous tensile strains. c) Differences in GF and strain range of DN hydrogel-based sensors from other sensors previously reported. d) Response time of DN hydrogel-based sensors under the transient deformation.

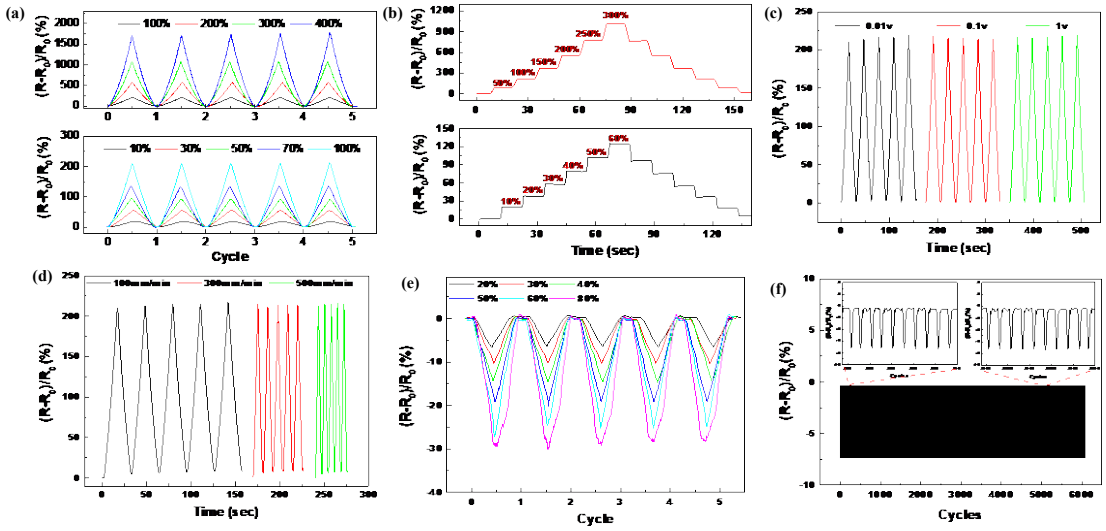

Fig. 4. The sensing performances of hydrogel a) under various cyclic tensile strains of 10%~100% and 100%~400%, b) under various tensile strains of 10%~60% and 50% ~300% (the strain was increased step-by-step, held for 10 s at every different strain), under cyclic stretching-releasing with a strain of 100% with c) different applied voltages (0.01 ~1V) and d) different stretching rates (100 ~ 500mm·min^{-1}), e) upon the periodical compression strain of 20% ~80%, f) durability test of sensor for 6000 compression cycles (The inserted Fig.s show the response signals of cycles 200-210, 5100-5110, respectively).

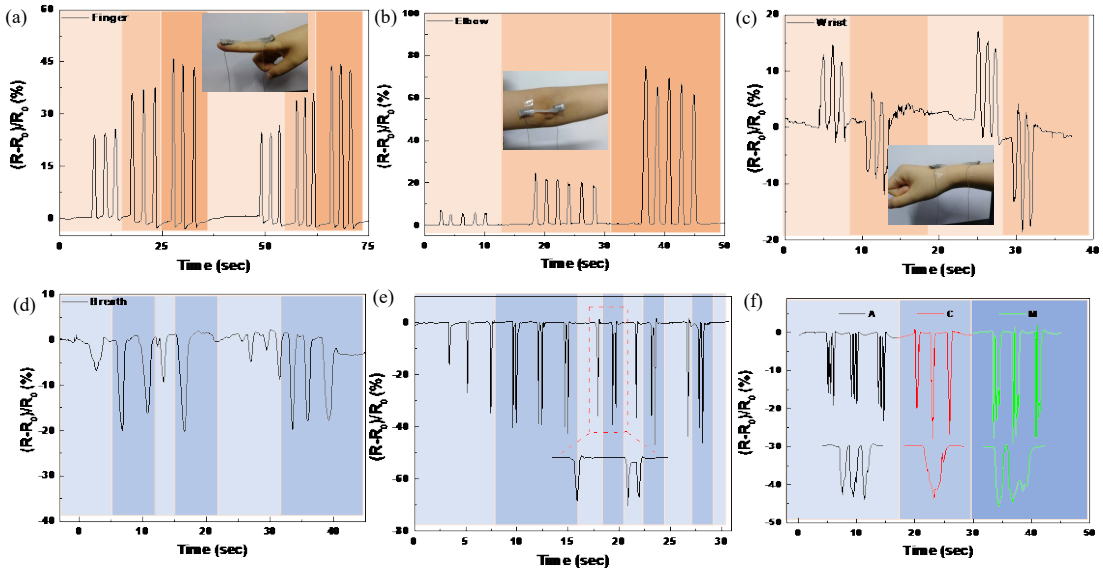

Fig. 5. The performance of hydrogel sensors for monitoring various human motions: the flexion of a) index finger and b) elbow, c) bent downward and upward of wrist and d) breathe monitoring. The responses of hydrogel sensors e) when the finger single-clicks and double-click on the surface and f) writing the letters of A, C and M on the surface with a pen.

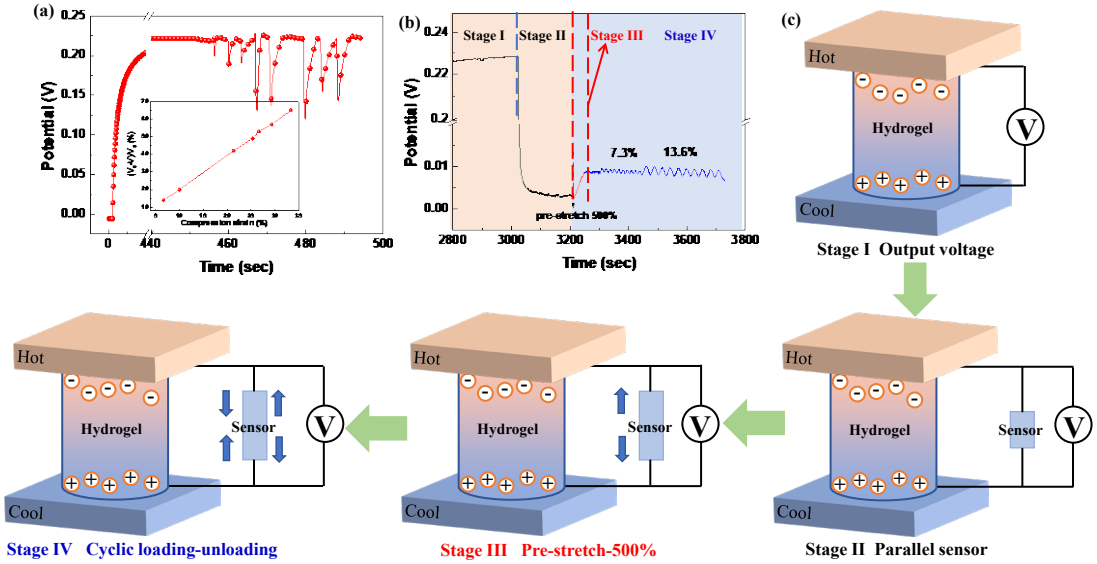

Fig. 6. a) The voltage variations of the hydrogel with ΔT of 7.5 K under different compressive strains. b) The voltage variations of the hydrogel sensor versus different tensile strains in parallel with thermoelectric hydrogels and c) the corresponding equivalent circuit diagram.